Fabrication of Silicon Carbide Nanocrystals by Electrical Discharge and Laser-Induced Processes in Solution

A. Nevar[1], N. Tarasenka[1], M. Nedelko[1], N. Tarasenko[1]*
Supriya Chakrabarti [2], Davide Mariotti[2]

Fabrication of Silicon Carbide Nanoparticles by Electrical Discharge and Laser-Induced Processes in Solution

[1]B. I. Stepanov Institute of Physics, National Academy of Sciences of Belarus,
68 Nezalezhnasti Ave., Minsk 220072, Belarus
[2] Nanotechnology & Integrated Bio-Engineering Centre, Ulster University, Newtownabbey, UK

* n.tarasenko@ifanbel.bas-net.by

ORCID
Alena Nevar https://orcid.org/0000-0001-9535-0385
Natalie Tarasenka https://orcid.org/0000-0001-7902-7932
Michail Nedelko https://orcid.org/0000-0001-7183-7367
Nikolai Tarasenko https://orcid.org/0000-0002-2222-9389
Supriya Chakrabarti https://orcid.org/0000-0001-5175-2884
Davide Mariotti https://orcid.org/0000-0003-1504-4383

Abstract

The capabilities of the liquid assisted electrical discharge techniques with additional laser irradiation of colloids for the synthesis of SiC nanocrystals (NCs) have been studied. For optimization of the conditions for the binary NCs formation, the characterization of inner structure, phase composition and morphology was performed by means of HRTEM, SAED, XPS, Raman and FTIR techniques. The results of the characterization proved the formation of near-spherical SiC nanocrystals with average diameter of 3.7 nm before and 2.3 nm after additional laser treatment. The possible mechanism of nanostructured SiC formation has been discussed from the point of thermodynamics. The developed technique is expected to be effective for fabrication of SiC NCs as a promising material for optoelectronic devices.

Keywords Silicon carbide nanoparticles, electrical discharge in liquid, laser irradiation, chemical interactions.

Declarations

Funding The work was partially financed by the National Academy of Sciences of Belarus under project Convergence 2.2.05 and by the Belarusian Foundation for Fundamental Researches under Grant No. F20KITG-008.

Conflicts of interest/Competing interests Not applicable

Availability of data and material Not applicable

Code availability Not applicable

Introduction

Plasma-chemical processes have proved to be attractive for the synthesis of nanoparticles (NPs) due to high production rates, versatility and possibility of control over the particle size and size distribution during the synthesis process. Different approaches based on non-thermal plasmas have been developed to adopt plasma processes to the NPs production depending on the required composition and structure [1-3]. These include nanoparticle formation in electrical discharge plasma ignited inside liquid between two electrodes, plasma in contact with liquid, as well as laser-induced plasma generated by focusing laser beam on the target surface in laser ablation experiments. Ignition of plasma favours initiation of the high temperature chemical reactions that provide the possibility of synthesis of metastable phases that are difficult to produce in other ways.

Silicon carbide is a wide bandgap semiconductor that is known for its high thermal stability that makes the SiC-based devices well-suited for high temperature operation conditions in which conventional semiconductors like silicon cannot perform adequately or reliably [1]. Besides, due to the high hardness and strength, chemical and thermal stability, high melting point, oxidation resistance, high erosion resistance and high thermal conductivity, SiC is especially promising for uses as heterogeneous catalyst support, for high power, high temperature electronic devices as well as abrasion and cutting applications [2]. However, because of the indirect band gap of bulk SiC its application in photonics and optoelectronics is restricted. Nevertheless, previous studies showed that nanostructured SiC provides photoluminescence at room temperature due to the formation of direct band gap and quantum confinement effect [4].

Previously, SiC nanostructures were shown to be fabricated by physical and chemical vapor deposition [5], reduction–carburization route [6], liquid phase sintering or mechanical alloying methods [7] and, recently, laser ablation technique [8]. However, the synthesis of SiC NCs still remains a challenge due to the high melting temperature and hardness of bulk silicon carbide. Therefore, the development of new approaches for the preparation of SiC NCs with pre-determined size, morphology and structure and increasing their photoluminescence is still of interest.

In this paper the capabilities of the electrical discharge in liquid (EDL) for preparation of SiC (NPs) are evaluated. Morphology, composition and structure of the synthesized NPs were studied by transmission electron microscopy (TEM), selected area electron diffraction (SAED), X-Ray photoelectron spectroscopy (XPS) and Fourier-transform infrared spectroscopy (FTIR). The optical properties of the synthesized NPs were analyzed by UV-Vis absorption and photoluminescence spectroscopy. Particles were found to be non-agglomerated and their size could be controlled via additional laser treatment. Different crystal structures were observed depending on the preparation procedure.

Experimental

To synthesize SiC NPs, electrical discharge between Si and C (graphite) electrodes immersed in ethanol were used. The details concerning the parameters of the experimental reactor and procedure of NPs synthesis by electrical discharge in liquids can be found in our previous publications [9, 10].

Briefly, the technique used for the synthesis of the SiC NPs utlized an electrical discharge submerged in liquid and is shown in the schematic diagram presented in Fig. 1a. An alternating current (ac) spark discharge was ignited by applying a high frequency voltage of 11 kV. The peak current of the high-voltage spark in the form of high-frequency oscillations was about 17 A with a duration of a single discharge pulse of 50 μs. The optimum distance between the electrodes (not more than 0.5 mm) during the experiment was controlled by micro positioning system maintaining the discharge parameters approximately constant to provide a stable discharge.

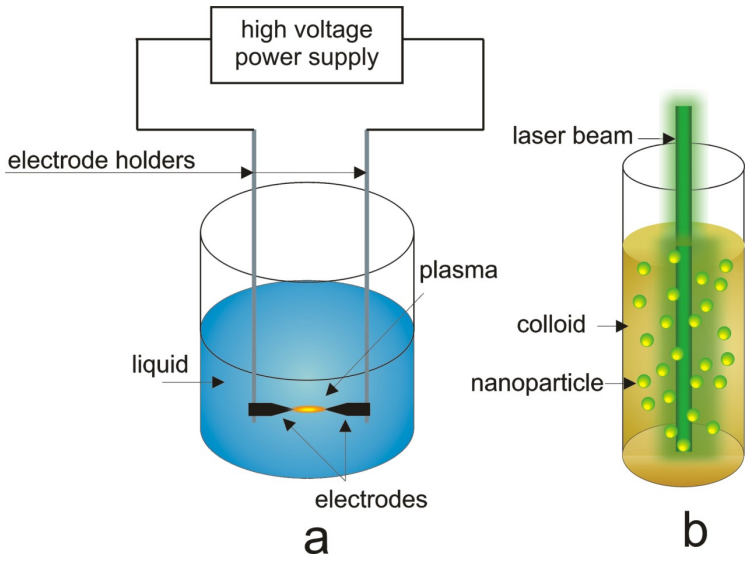

Fig. 1 Schematic diagram representing the techniques used for SiC NPs preparation: (a) electrical discharge between silicon and graphite electrodes in ethanol and (b) laser irradiation of the as-prepared by EDL colloidal solution

After the preparation the colloids, these were further irradiated by an unfocused beam of the second harmonic of an Nd:YAG laser (532 nm) with pulse duration 10 ns, repetition rate 10 Hz, fluences in the range of 230 – 600 mJ/cm^2.

The phase composition, morphology and structure of the synthesized NPs were analyzed by HRTEM, SAED, XPS, FTIR techniques along with UV-Vis absorption and photoluminescence spectroscopy. The particle size and morphology were investigated by the transmission electron

microscope JEOL JEM-2100F (JEOL, USA) operating under accelerating voltage of 200 kV. For TEM and SAED measurements, the NPs were deposited onto the copper grids covered by Formvar films stabilized with carbon and dried at ambient conditions. Crystal structure, phase composition and lattice parameters of the formed SiC nanostructures were determined from SAED and HRTEM images analysis by fast Fourier transform (FFT). For FTIR and XPS measurements the colloidal solution was deposited on Al foil and dried at room temperature. The FTIR spectra were recorded by Fourier spectrometer Nexus (Termo Nicolet, USA) in the 4000 – 400 cm^{-1} region. The absorption spectra of the prepared colloids were measured using a Cary 500 Scan spectrophotometer (Varian, USA) in the spectral range 200–800 nm using quartz 10 mm cuvette. The photoluminescence measurements were carried out at room temperature using a spectrofluorimeter Solar SFL 1211A (Solar, Belarus) with a Xe lamp as an excitation source.

Results and discussions

The electrical discharge between Si and C electrodes in ethanol results in the formation of near-spherical NPs with a size distribution that presents two peaks as can be concluded from the TEM results, shown in Fig. 2a. This is the result of particles agglomeration where small and well-separated NPs with an average diameter of 3.7 nm were found together with agglomerates with an average diameter of 11.4 nm (Figs 2a-b). HRTEM analysis of the selected particles revealed lattice spacings close to 0.25 nm (Fig. 2c), which belongs to the (111) planes of 3C-SiC with a cubic unit cell parameter of 0.43591 nm [11]. It is known that SiC exhibits strong polytypism with several crystalline structures and varying stacking sequences, the most widespread and important of them result from pure cubic (β) stacking (3C-SiC) and hexagonal (α) stacking (specifically, 4H-SiC and 6H-SiC) [12]. Among all the structures, the β-SiC phase is known to be the most stable. The determined lattice spacing values and plane assignments are confirmed by FFT of the corresponding high resolution images (Fig. 2d). The observations support the assignment of a cubic crystal structure as more probable and stable than the hexagonal one. It should be noted that minor reflections corresponding to cubic Si and carbon with graphite-like structure were also observed in the prepared sample.

Additional laser treatment results in the transformation of the size distribution as can be concluded from Figures 2e-f. Most probably, large agglomerates undergo fragmentation due to the absorption of the laser pulses that results in the disappearing of the second peak in the size distribution and reduction of the average particles diameter down to 2.3±0.1 nm.

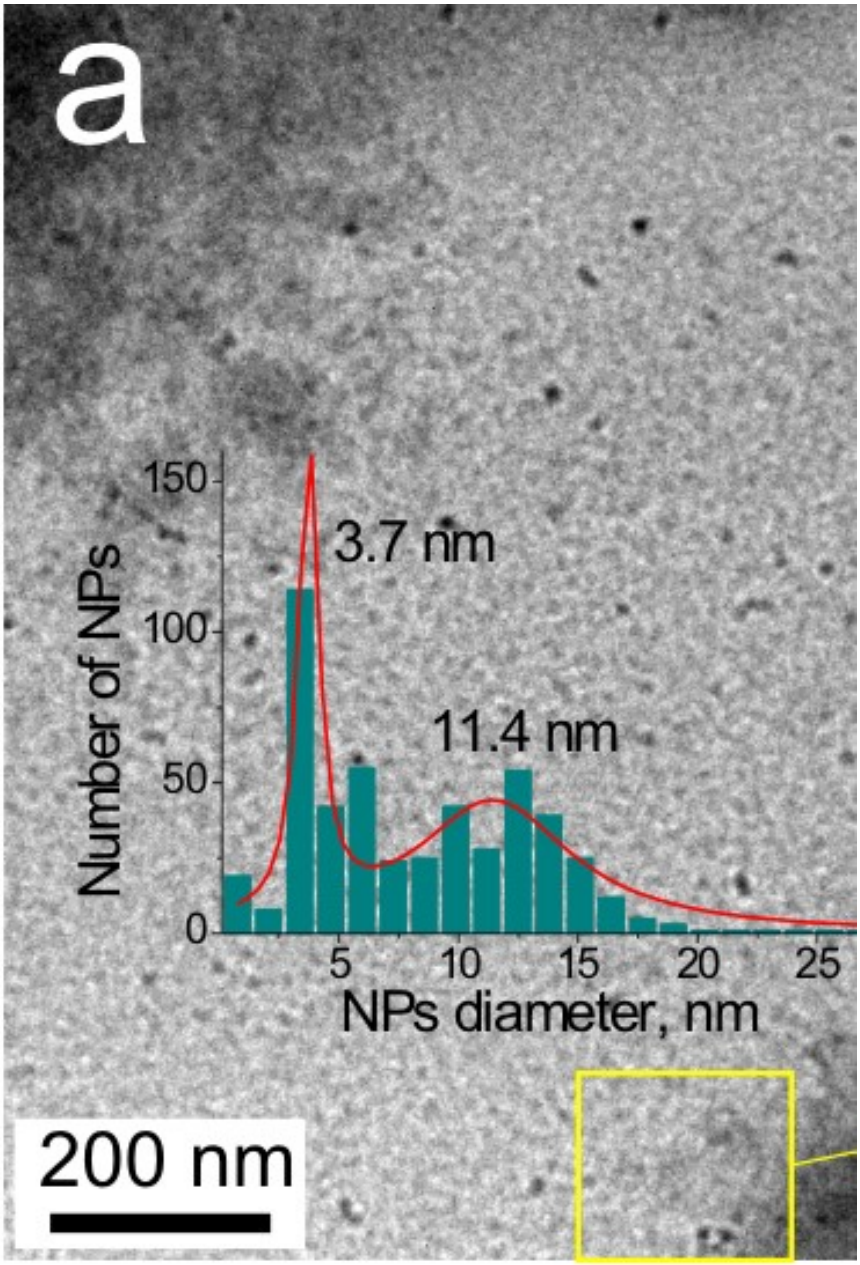

Fig. 2. SiC NPs prepared by electrical discharge in ethanol: a, b – TEM images of NPs with different resolutions and with the corresponding size distribution fitted by two peak function shown in the inset; c – HRTEM of a single particle showing the interplanar spacing corresponding to (111) plane of cubic SiC; d – FFT of the corresponding HRTEM revealing the minor cubic Si phase present in the sample; e – TEM image of SiC NPs after irradiation with 532 nm ns laser with fluence 560 mJ/cm^2, f – size distribution of the NPs in the irradiated SiC sample. The mean diameter of the particles found from the lognormal fit of the distribution was 2.3±0.1 nm

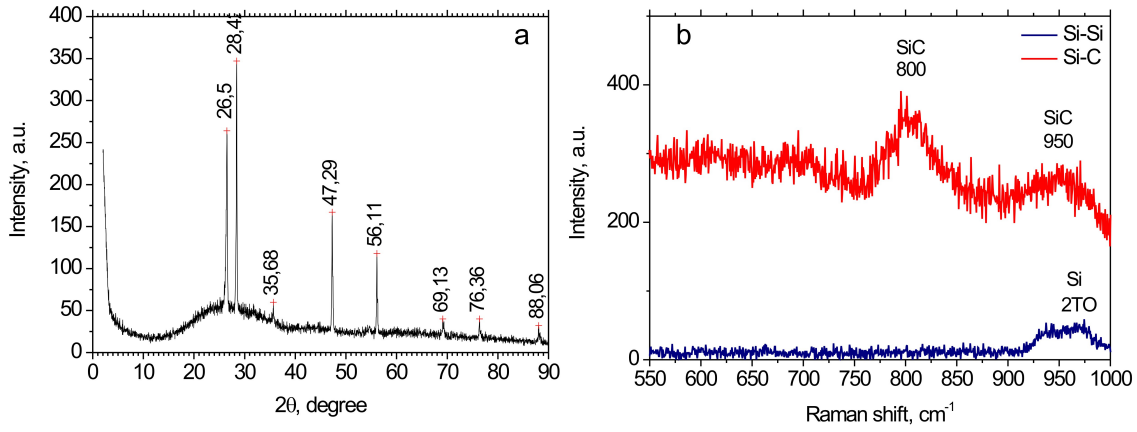

Fig.3. XRD pattern of NPs prepared by Si−C electrical discharge in ethanol (a) and Raman spectra of the samples prepared by the Si−C and Si−Si discharges in ethanol (b).

The cubic crystalline structure of the formed SiC NCs was also confirmed by X-ray diffraction analysis (Fig. 3a), although, as it was previously discussed [13], determination of a polytype from XRD spectrum is difficult in many cases. Nevertheless, the presence of the peaks located at 2θ = 35.7˚ and 60.4˚ corresponding to the reflection from the (111) and (220) crystal planes indicated a formation of the SiC cubic phase (JCPDS card No. 29-1129). In addition to the defined SiC structure, some diffraction peaks attributable to the pure Si with cubic structure and C of hexagonal graphite structure were also observed in the XRD pattern. More pronounced diffraction peaks of Si and C particles compared to SiC ones can be reflected the smaller size and a presence of structural defects in the formed SiC NCs. It should be noted that the discharge parameters and time of discharge processing can be optimized to avoid the presence of the initial unreacted particles in the resulting samples.

Raman analysis also showed the presence of SiC in the sample prepared by electrical discharge between Si and C electrodes in ethanol. The spectrum of the sample prepared by spark discharge between two silicon electrodes using the same parameters is shown for comparison. In the spectrum of the latter a broad band at around 950-970 cm^{-1} was observed that can be attributed to the second order transverse optical mode in silicon nanocrystals [14]. In contrast, in the sample prepared using silicon and carbon electrodes, two peaks centred at around 800 cm^{-1} and 950 cm^{-1} appear which correspond to the transverse optical (TO) and longitudinal optical (LO) modes in cubic SiC [15]. The peaks were found to be broadened and shifted with respect to the bulk values (770 and 888 cm^{-1}) [16] that can be attributed to the decrease of grain size and formation of defects in the silicon carbide structure [17].

Further evidence for the composition of the synthesized NPs was obtained by FTIR and XPS results that support the TEM, XRD and Raman analysis suggesting the formation of SiC NPs. Indeed, the peak at around 796 cm^{-1} found in the FTIR of the samples (Fig. 4) can be attributed to the stretching vibrations of the Si-C bonds [18]. In addition, the particles can be coated with the C–H groups as the peaks at 2846, 2910 and 2958 cm^{-1} corresponding to the C–H stretching vibrations were found (Fig. 4). Besides, the particles are oxidized as the broad peak around 1000-1100 cm^{-1} may be attributed to the stretching vibrations of the Si–O–Si, Si–O–C or C–O–C groups that is consistent with the XPS results shown below. The formation of oxygen-containing groups may be the result of particles interaction with ethanol or products of ethanol decomposition. Otherwise, they can be formed after particles deposition and drying during FTIR samples preparation procedure. Additional laser processing of the colloids results in the increase of the particles oxidation as the intensity of the broad band at 1000-1100 cm^{-1} increases. Besides, the band corresponding to the stretching vibrations of O–H group also appears at around 3300 cm^{-1}.

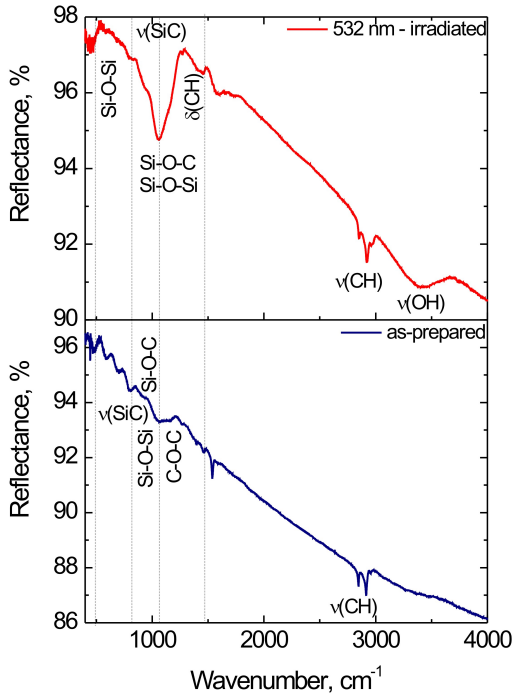

Fig: 4. FTIR analysis of the SiC NPs prepared by electrical discharge in ethanol before and after laser irradiation, revealing the vibrations of Si-C at 796 cm^{-1}.

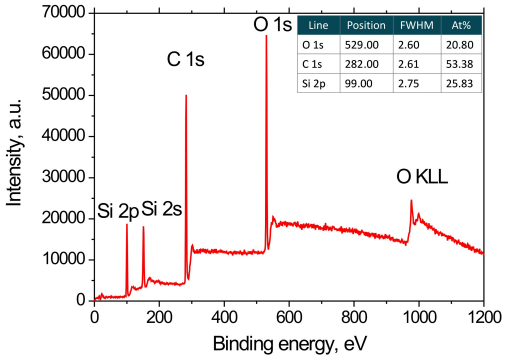

Fig: 5. XPS spectrum of the SiC sample, the inset table shows the results of the composition evaluation based on the XPS results.

The XPS analysis of the sample prepared by discharge in ethanol reveals that the sample consists only of Si, C and O atoms with the atomic ratio Si:C:O=25.83 : 53.38 : 20.80 (Fig. 5). The analysis of the high-resolution XPS profiles for the Si 2p, C 1s and O 1s lines is presented in the Fig. 6.

The position of the silicon Si 2p line in the XPS spectra of the samples suggests the formation of the silicon carbide phase as its maximum is located at 101.2 eV, close to 101.5 eV reported for the high-coordinated Si-C bonds [19]. The XPS profile however show extensive oxidation with bonds at around 101.7 eV [18-20] coming from the admixture of silicon oxycarbides. It should be noted that the peak in the region 102.2 eV attributable to the Si-O bond was found to be significantly lower in comparison with the first two peaks [18-20].

The high-resolution XPS spectra from Si 2p line of the laser-irradiated sample shows similar features to the not-irradiated one. As seen from the comparison of the Figs. 6a and 6c, the spectra are deconvoluted into the profiles corresponding to the high-coordinated Si-C (101.25 eV), Si-C-O (101.67 eV) and Si-O (102.17 eV) bonds. In addition, a low-coordinated Si-C peak could also be fitted in thie case at 100.89 eV.

Thus, the XPS results evidence that laser treatment does not affect significantly the chemical state of the NPs surface, but results in reduction of the average particles size as it follows from the TEM observations.

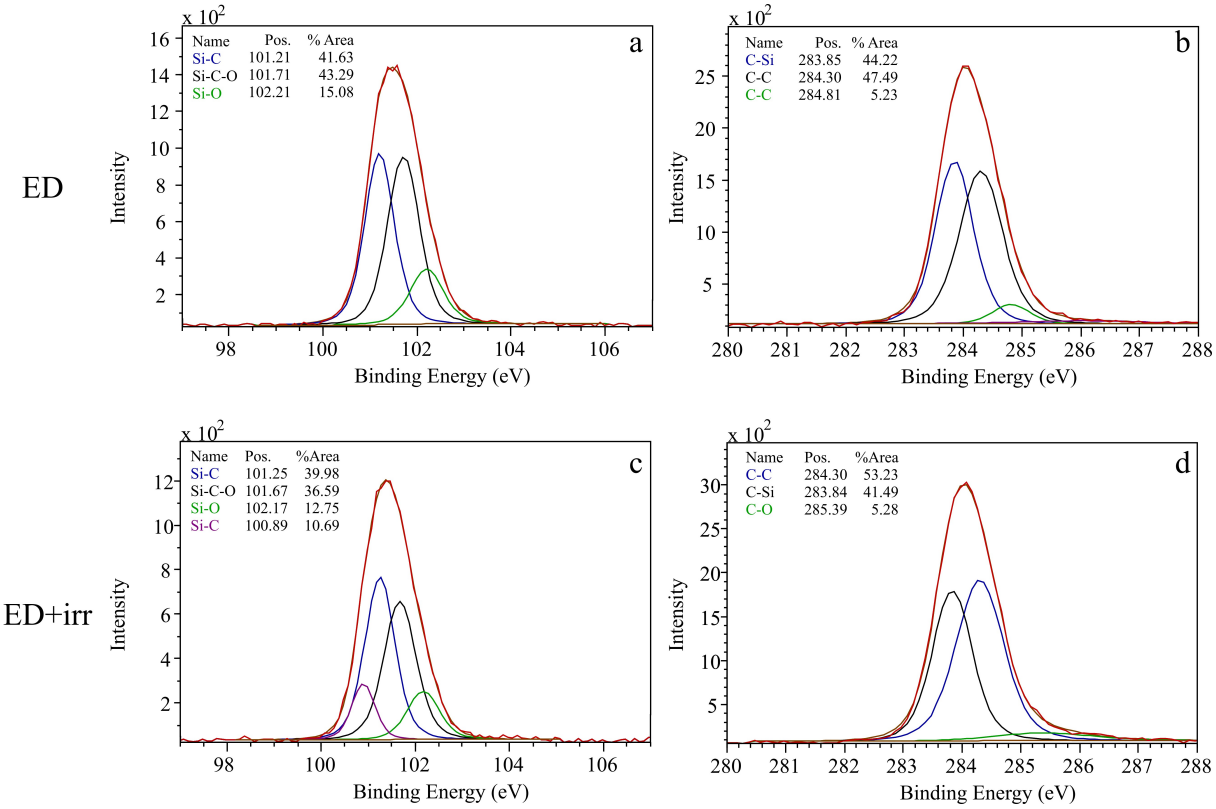

Fig: 6. High resolution XPS profiles of Si 2p (a, c) and C 1s lines (b, d), respectively. The observation of Si 2p peak at 101.2 eV gives the evidence of the Si-C bonds formation.

The UV-Vis absorption spectra of the SiC NPs synthesized by electrical discharge technique are shown in Fig.7a. The absorption spectrum of the SiC colloids exhibits a step-like behaviour with a sharp rise when the incident photon energy is larger than 3 eV. Above the band gap (~3 eV), a strong continuous increase of absorption is observed in the spectrum.

The mechanism of absorption in these two regions – below and above the bandgap – are explained by the absorption by band tail states in the first case, and by the band-band transitions in different NCs above the bandgap [21]. In addition, the absorption peaks at 4.5 and 4.8 eV were observed and can be attributed to the confined energy levels of small cubic SiC NPs [21].

The optical absorption spectra allow estimating the bandgap of the SiC NCs using Tauc plots and taking into account that SiC NCs have indirect bandgap characteristics [21]. The bandgap values determined from the Tauc plot of as-prepared sample was found to be in the range 2.5-3.5 eV, while for the laser irradiated sample this range was estimated to be 3.0-3.6 eV that can be attributed to the narrowing of the particles size distribution after laser treatment and fragmentation of the particles with diameters larger than 10 nm. In both cases the obtained bandgap values are above the bulk

value (E_g = 2.36 eV for 3C-SiC polytype) [22] that can be related to quantum confinement effects in the prepared particles due to the size reduction.

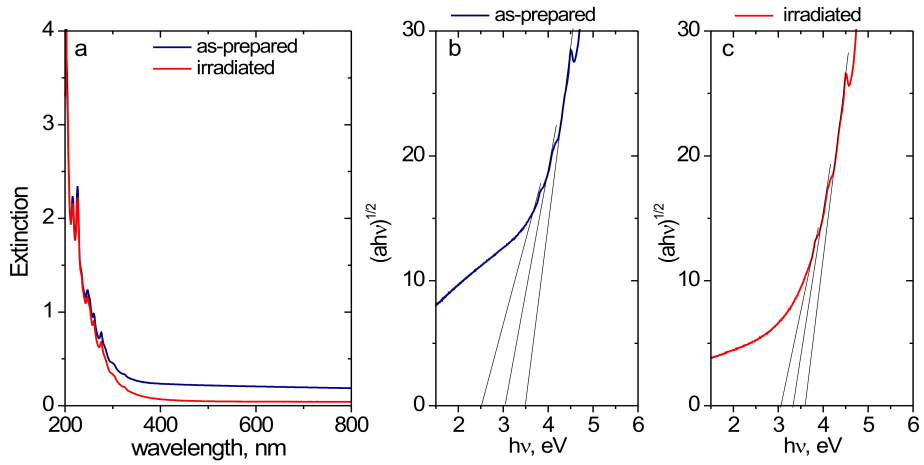

Fig. 7. UV-Vis absorption spectra (a) and Tauc plots used for bandgap estimation of as-prepared (b) and laser irradiated SiC NPs (c)

We compared the determined value of the bandgap with an estimated one according to the equation [23]

$$E_{NP}(d) = E_{bulk} + \frac{h^2}{2d^2}\left(\frac{1}{m^*_e} + \frac{1}{m_h^*}\right) - \frac{1.8e^2}{2\pi\varepsilon_d\varepsilon_0 d}$$

where h is Planck's constant, e the electron charge, ε_0 the vacuum permittivity and d the particle diameter. Using literature values for the bulk bandgap (2.36 eV), effective electron mass m_e^* ($0.347m_0$), effective hole mass m_h^* ($0.45m_0$) and dielectric constant of bulk SiC (ε_d = 9.52) [24] it was found that the bandgap for SiC NCs with diameters of 2.4-7.0 nm is in the range 3.5-2.5 eV that is in good agreement with the measured bandgap values (Fig. 2). For the laser irradiated sample having the average particle diameter 2.3 nm (Fig. 2f) the calculated bandgap is 3.6 eV that lies in the range of the estimated values from the Tauc plot (Fig. 7c).

Due to the quantum confinement the photoluminescent properties of the small SiC NCs are different from the bulk ones. As can be seen from Fig. 8 the room temperature PL spectrum of the SiC NCs prepared by the electrical discharge in ethanol reveals rather narrow emission band with a maximum in the region of 410 nm. The PL emission of SiC NPs can be originated from bandgap transitions or transitions from defect states and surface terminations [25]. The maximum of the PL band can be attributed to the band edge luminescence of the small SiC NCs as it is consistent with the determined increased bandgap for small NCs bandgap (3.0 eV).

After laser irradiation, the intensity of the PL emission band increases while its position does not change (Fig. 7b). In addition, the band broadens as the shoulder at around 450-550 nm appears that

may be indicative of the formation of different emission centers under laser treatment. Typically, the broadening of the luminescence spectrum of silicon carbide nanostructures is attributed either to the size distribution of the particles in the sample, to the formation of defects or difference in the surface groups. However, in the present case the observed narrowing of the size distribution after the laser treatment makes the first mechanism improbable. Besides, according to the FTIR and XPS analysis, additional laser irradiation results in the oxidation of the particles surface with the formation of Si–C–O, Si–O–Si and C–O–C groups. Therefore, it can be assumed that the new luminescence centers created upon laser treatment can be attributed to the particles oxidation with the formation of the additional levels near the edges of the valence and conduction bands of the SiC structure that are responsible for the transitions in the 450-550 nm region [26].

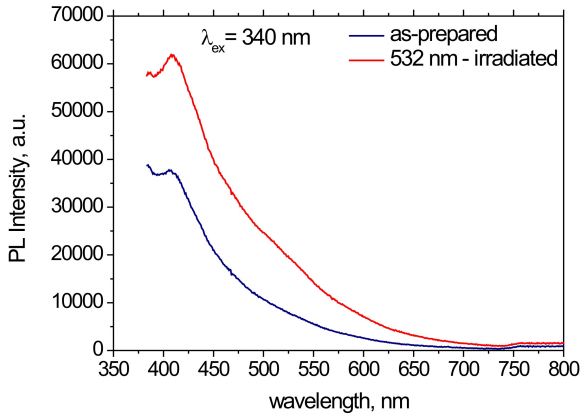

Fig. 8. Photoluminescence spectra (excited at 340 nm) of SiC NCs prepared by electrical discharge in ethanol as-prepared and after additional laser irradiation

Although the exact mechanism of SiC growth in plasma of electrical discharge in liquid is unknown, we can suggest several routes. It is generally considered that the mechanism of the particles formation in electrical discharge plasma implies the evaporation of the electrode material with subsequent condensation of the formed species into small clusters, their aggregation and formation of particles [27]. NPs are formed from the atoms and their gaseous complexes as a result of a sequence of nucleation, growth, coalescence and aggregation processes. Silicon and carbon atoms, formed by the evaporation of the electrodes, are initial species in this sequence. The presence of silicon and carbon atoms and their dimers in the discharge plasma was confirmed by spectroscopic studies (Fig. 8), the results of which concluded that the discharge takes place in a gas mixture consisting of atoms of the electrode material and products of ethanol decomposition [9]. In addition, in the 390-420 nm region of the emission spectrum of the Si-C discharge some weak lines can be ascribed to the band heads of bands of C_2-X and $C^3\Pi$-$X^3\Pi$ systems of SiC molecule that also can be a possible route for SiC particles formation and nucleation [28].

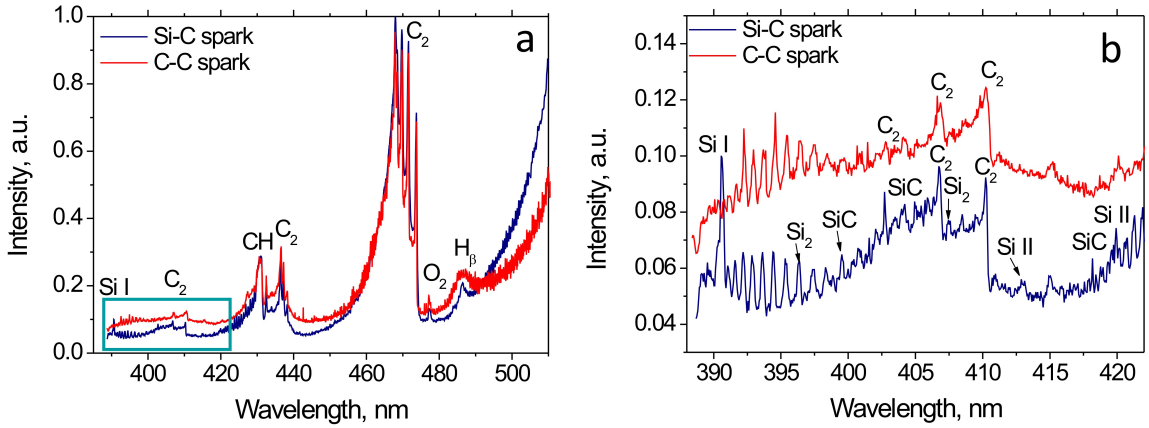

Fig. 8. Optical emission spectra (OES) of the plasma generated during the spark discharge between the Si and C electrodes immersed in ethanol (blue lines) and between graphite electrodes in ethanol (red lines, shown for comparison (a). (b) – a closer look at the region 390-420 nm

From the viewpoint of thermodynamics, the formation of new compounds should occur as a result of collisions between the species in relatively high-energy states, while the nucleation may result from aggregations of the formed species [29]. By expanding and intermixing of the species of both materials, e.g., atoms, ions, and/or small clusters a dense two-component cloud is formed in the space between electrodes. An interaction between the ablated species can result in the SiC compounds formation. As it follows from the Si-C equilibrium phase diagram [30] the critical SiC nuclei could form in the temperature range of 1800–2000 K. Such thermodynamic conditions can be created by electrical discharge in liquid. Indeed, according to [9,10] the temperature and pressure within the reaction volume can be extreme (thousands of K at tens of MPa). Thus, the solution plasma can provide the compound NPs formation through the mechanism of the primary nucleation in the plasma plume of the Si and C atoms evaporated from the electrodes and growth of the embryonic particles. The crystallization process is believed to be closely linked to efficient heating of NPs through interaction with charged plasma species, i.e. due to ion and hot electron surface bombardment during growth [31]. When the particles escape from the plume into the liquid media, they become cold rapidly and the growth process is suppressed via reactive quenching with solution where Si-C, Si-CH_3 or C=O bonds can be formed on the particle surface.

Conclusion

Nanocrystalline particles of silicon carbide were synthesized by electrical discharge between Si and C electrodes immersed in ethanol. The NPs size and crystal structures were found to be changed after the additional laser irradiation of the formed colloidal solution. The formation of

compound SiC NCs was confirmed by the results of their characterization with the HRTEM, XPS, and FTIR measurements. The fabrication of SiC NCs with the dimensions less 10 nm having a cubic (3C-SiC) internal structure was observed.

From practical point of view the approach based on electrical discharge in liquid seems attractive because it provides scalable and suitable for high volume production process. The additional laser treatment of colloidal mixture also offers interesting possibilities as the second step for the controlled modification of NPs synthesized via electrical discharge. The developed technique can be optimized to prepare SiC NCs satisfying the requirements of good dispersibility, stability and effective PL for practical applications, for example, as elements for next generation quantum sensing and nanophotonics, light emitting diodes and photodetectors.

References

1 Abderrazak H, Bel Hadj Hmida E S (2011) Silicon Carbide: Synthesis and Properties in Properties and Applications of Silicon Carbide, ed. Rosario Gerhardt. InTech. DOI: 10.5772/15736

2 Wu R, Zhou K, Yue C Y, Wei J, Pan Y (2015) Recent progress in synthesis, properties and potential applications of SiC nanomaterials. Progr. in Mater. Sci. 72:1-60

3 Castellazzi A, Fayyaz A, Romano G, Yang L, Riccio M, Irace A (2016) SiC power MOSFETs performance, robustness and technology maturity. Microelectronics Reliability 58:164-176

4 Cao T, Cheng Y, Zhang H, Yan B, Cheng Y (2015) High rate fabrication of room temperature red photoluminescent SiC nanocrystals. J.Mater.Chem.C3: 4876–4882.

5 Stenberg P, Booker ID, Karhu R, Pedersen H, Janzén E, Ivanov IG (2018) Defects in silicon carbide grown by fluorinated chemical vapor deposition chemistry. Physica B: Condensed Matter. 535: 44-49

6 Hu JQ, Lu QK, Tang KB, Deng B, Jiang RR, Qian YT, Yu WC, Zhou GE, Liu XM, Wu JX (2000) Synthesis and characterization of SiC nanowires through a reduction-carburization route. J. Phys. Chem. B 104:5251-5254

7 Izhevskyi VA, Genova LA, Bressiani AHA, Bressiani J C (2000) Liquid Phase Sintered SiC. Processing and Transformation Controlled Microstructure Tailoring. Mat. Res. 3: 131-138

8 Askari S, Macias-Montero M, Velusamy T, Maguire P. Svrcek V, Mariotti D (2015) Silicon-based quantum dots: synthesis, surface and composition tuning with atmospheric pressure plasmas. Journal of Physics D: Applied Physics 48: 314002

9 Nevar AA, Kiris VV, Mardanian MM, Nedelko MI, Tarasenko NV (2016) Synthesis of silicon nanocrystals in electrical discharge in liquid with spectroscopic plasma characterization. High Temp. Mater. Processes 20: 251–265

10 Mardanian M, Nevar AA, Tarasenko NV (2013) Optical Properties of Silicon Nanoparticles Synthesized via Electrical Spark Discharge in Water. Appl. Phys. A. 112:437–442

11 Iwanowski RJ, Fronc K, Paszkowicz W, Heinonen M (1999) XPS and XRD study of crystalline 3C-SiC grown by sublimation method. J. Alloys Compd. 286:143–147

12 Andrievski RA (2009) Synthesis, structure and properties of nanosized silicon carbide. Rev.Adv.Mater.Sci. 22:1-20

13 Zekentes K, Rogdakis K (2011) SiC nanowires: material and devices. J. Phys. D: Appl. Phys. 44: 133001

14 Mercaldo LV, Esposito EM, Delli Veneri P, Fameli G, Mirabella S, Nicotra G (2010) First and second-order Raman scattering in Si nanostructures within silicon nitride. Appl. Phys. Lett. 97:153112

15 Wieligor M, Yuejian Wang Y, Zerda TW (2005) Raman spectra of silicon carbide small particles and nanowires. J. Phys.: Condens. Matter 17:2387–2395.

16 Meng A, Zhang M, GaO W, Sun S, Li Z (2011) Large scale synthesis of β-SiC nanochains and their Raman/photoluminescence properties, Nanoscale Res. Lett. 6:1–7.

17 Vetter WM and Dudley M (2004) Characterization of defects in 3C-silicon carbide crystals. J. Cryst. Growth 260:201-208.

18 Wang L, Xu J, Ma T, Li W, Huang X, Chen K (1999) The influence of the growth conditions on the structural and optical properties of hydrogenated amorphous silicon carbide thin films. J. Alloys Compd. 290:273-278

19 Askari S, Ul Haq A, Macias-Montero M, Levchenko I, Yu F, Zhou W, Ostrikov K, Maguire P,. Svrcek V and Mariotti D (2016) Ultra-small photoluminescent silicon-carbide nanocrystals by atmospheric-pressure plasmas. Nanoscale 8:17141

20 Kim M, Kim J (2014) Development of high power and energy density microsphere silicon carbide–MnO_2 nanoneedles and thermally oxidized activated carbon asymmetric electrochemical supercapacitors. Phys.Chem.Chem.Phys 16:11323-11336

21 Li Y, Chen C, Li J.-T, Yang Y and Lin Z-M (2011) Surface charges and optical characteristic of colloidal cubic SiC nanocrystals. Nanoscale Res. Lett. 6:454

22 Fan J, Chu P K (2014) Silicon Carbide Nanostructures: Fabrication, Structure, and Properties. Springer, Switzerland

23 Brus, L. Electronic Wave Functions in Semiconductor Clusters: Experiment and Theory. *J. Phys. Chem.* **1986**,*90* (12), 2555–2560. https://doi.org/10.1021/j100403a003

24 Madelung, O. *Semiconductors: Data Handbook*, 3rd ed.; Springer Berlin Heidelberg, 2004. https://doi.org/10.1007/978-3-642-18865-7

25 Dai D, Guo X, Fan J (2015) Identification of luminescent surface defect in SiC quantum dots Appl. Phys. Lett. 106: 053115

26 Beke D, Szekrényes Z, Czigány Z, Kamarása K and Gali Á (2015) Dominant luminescence is not due to quantum confinement in molecular-sized silicon carbide nanocrystals. Nanoscale 7: 10982

27 Kabbara H, Noël C, Ghanbaja J, Hussein K, Mariotti D, Švrček V, Belmonte T (2015) Synthesis of nanocrystals by discharges in liquid nitrogen from Si–Sn sintered electrode. Sci. Rep. 5:17477

28 Ojha K S, Gopal R (2011) New Band Systems of SiC Molecule in Visible Region. Spectrosc. Lett. 44:267–272

29 Yang G W (2007) Laser ablation in liquids: Applications in the synthesis of nanocrystals. Progress in Materials Science 52: 648-698

30 Haase V, Kirschstein G, List H, Ruprecht S, Sangster R, Schröder F, Töpper W, Vanecek H, Heit W, Schlichting J, Katscher H (1985) The Si-C Phase Diagram. In: Katscher H, Sangster R, Schröder F. (eds) Si Silicon. Gmelin Handbook of Inorganic Chemistry, vol S-i /B/1-5/3. Springer, Berlin, Heidelberg

31 Askari S, Levchenko I, Ostrikov K, Maguire P, Mariotti D (2014) Crystalline Si nanoparticles below crystallization threshold: effects of collisional heating in non-thermal atmospheric-pressure microplasmas. Appl. Phys. Lett. 104:163103